Ecotoxicology and Environmental Safety 196 (2020) 110511

Contents lists available at ScienceDirect

Ecotoxicology and Environmental Safety

journal homepage: www.elsevier.com/locate/ecoenv

Accumulation of ^{13}C-labelled phenanthrene in phytoplankton and transfer to corals resolved using cavity ring-down spectroscopy

Ananya Ashok[a,*], Sreejith Kottuparambil[a], Lone Høj[c], Andrew P. Negri[c], Carlos M. Duarte[a,b], Susana Agustí[a]

[a] Red Sea Research Center (RSRC), King Abdullah University of Science and Technology (KAUST), Thuwal, 23955-6900, Saudi Arabia
[b] Computational Bioscience Research Center (CBRC), King Abdullah University of Science and Technology (KAUST), Thuwal, 23955-6900, Saudi Arabia
[c] Australian Institute of Marine Science (AIMS), Townsville, 4810, Queensland, Australia

ARTICLE INFO

Keywords:
PAHs
Phenanthrene
Stable isotopes
Bioaccumulation
Corals
Phytoplankton

ABSTRACT

Polycyclic aromatic hydrocarbons (PAHs) are widespread pollutants in marine ecosystems including threatened and potentially sensitive coral reefs. Lower organisms such as phytoplankton, known to bioconcentrate PAHs, could serve as potential entry points for these chemicals into higher trophic levels. Here, we present a novel method using a ^{13}C-labelled PAH and cavity ring-down spectroscopy (CRDS) to investigate accumulation, uptake rates and trophic transfer of PAHs in corals, which are key organisms to sustain biodiversity in tropical seas. We quantified the accumulation of ^{13}C-phenanthrene in the marine microalga *Dunaliella salina*, and in the coral *Acropora millepora* after diffusive uptake from seawater or dietary uptake via labelled *D. salina*. Additionally, we monitored the photophysiological health of *D. salina* and *A. millepora* during phenanthrene exposure by pulse-amplitude modulation (PAM) fluorometry. Dose-dependent accumulation of ^{13}C-phenanthrene in the microalga showed a mean bioconcentration factor (BCF) of 2590 ± 787 L kg^{-1} dry weight. Corals accumulated phenanthrene from both exposure routes. While uptake of ^{13}C-phenanthrene in corals was faster through aqueous exposure than dietary exposure, passive diffusion showed larger variability between individuals and both routes resulted in accumulation of similar concentrations of phenanthrene. The ^{13}C-PAH labelling and analysis by CRDS proved to be a highly sensitive method. The use of stable isotopic label eliminated additional toxicity and risks by radioactive isotopic-labelling, and CRDS reduced the analytical complexity of PAH (less biomass, no extraction, fast analysis). The simultaneous, precise quantification of both carbon content and ^{13}C/^{12}C ratio (δ^{13}C) enabled accurate determination of ^{13}C-phenanthrene accumulation and uptake rate. This is the first study to provide empirical evidence for accumulation of phenanthrene in a phytoplankton-coral food chain.

1. Introduction

Coral reefs are under threat from a range of anthropogenic pressures that include ocean warming and acidification (Hughes et al., 2017) as well as pollution (Kennish, 2017). Corals are vulnerable to the impacts of oil pollution from accidental spills at extraction facilities and from shipping in close proximity to tropical reefs (Kroon et al., 2019; Loya and Rinkevich, 1980). Polycyclic aromatic hydrocarbons (PAHs) are considered the most toxic components of oil to aquatic species, with the low molecular weight PAHs (2–3 rings) often posing the greatest hazard due to their higher solubility and relative abundance in many oil types (French-McCay, 2002; Redman and Parkerton, 2015).

The primary toxic mode of action of PAHs in aquatic organisms is narcosis, due to accumulation in- and disruption of-lipid membranes (Di Toro et al., 2000). PAHs dissolved in seawater can cause a variety of negative effects to corals ranging from tissue damage to bleaching, mortality and inhibition of larval settlement (Negri et al., 2016; Nordborg et al., 2018; Overmans et al., 2018; Peters et al., 1981; Renegar et al., 2017; Turner and Renegar, 2017). Also, by accumulating in phytoplankton, which present large surface to volume ratios for absorption, PAHs can enter into the lowest trophic level of marine food-webs (Fan and Reinfelder, 2003; Koelmans, 2014). Accumulation of PAHs via ingestion of contaminated food including phytoplankton are well described in some organisms like marine copepods (Arias et al., 2016; Berrojalbiz et al., 2009; Wang and Wang, 2006). Yet, toxic manifestations of PAHs acquired through dietary exposure are not well known (Wang et al., 2017). As for corals, there is very little information on pathways of PAH incorporation, although corals of the genus

* Corresponding author.
E-mail address: ananya.ashok@kaust.edu.sa (A. Ashok).

https://doi.org/10.1016/j.ecoenv.2020.110511
Received 2 December 2019; Received in revised form 16 March 2020; Accepted 17 March 2020
Available online 01 April 2020

Acropora have been shown to accumulate PAHs, inferred to be derived from both seawater and feeding in their natural environments (Jafarabadi et al., 2018; Xiang et al., 2018; Yang et al., 2019). Some corals are also known to retain PAHs in their tissues over prolonged periods (Knap et al., 1982; Peters et al., 1981; Solbakken et al., 1984). While ingestion has been identified as the more important route of PAH uptake in filter feeding organisms (Bresler et al., 1999), corals have a large surface area, and accumulation though passive diffusion is also likely. Despite these observations, studies examining pathways of PAH accumulation in corals are scarce mainly due to the limitations of available analytical methods.

Carbon stable-isotope (^{13}C) labelling and quantification through cavity ring-down spectroscopy (CRDS) could overcome major limitations of methods typically used to study accumulation of persistent organic pollutants. For instance, radioactive tracers used (Björk and Gilek, 1996; Jensen et al., 2012; Spann et al., 2015) can pose additional toxicity risks and require separate quantification based on activity. Alternatively, stable isotope-labelled compounds allow simultaneous measurement of mass and isotopic abundance, with precise quantification up to individual atoms (Bier, 1997; Graham et al., 2010). ^{13}C-labelled phenanthrene addition has been used to examine PAH behavior in soils (Bernard et al., 2007; Cennerazzo et al., 2017; Richnow et al., 1998), but we are unaware of similar studies using ^{13}C-labelled PAHs in marine ecosystems. A possible reason may be the high cost and technical complexity of Isotope Ratio Mass Spectrometry (IRMS) instruments and procedures, typically used to resolve ^{13}C-labelled pollutants.

Advent of the CRDS method has greatly reduced the cost and complexity of carbon cycling assessments (Maher et al., 2013), recently displacing both radioisotope labelling and IRMS-based ^{13}C-labelled techniques for marine applications (López-Sandoval et al., 2019). The application of CRDS therefore offers a promising yet untested method to assess ^{13}C-labelled pollutant accumulation and transfer in marine food webs. In this paper, we describe experiments examining the toxicity and accumulation of the PAH, ^{13}C-phenanthrene, using the novel CRDS analytical approach in a one-step experimental marine food chain involving the microalga *Dunaliella salina* and the widely-distributed coral, *Acropora millepora*. Our study contributes to understanding trophic transfer of PAHs in tropical marine organisms for which information is scarce while highlighting the efficacy of CRDS as a tool to resolve uptake and transport of persistent organic pollutants in marine ecosystems.

2. Materials and methods

2.1. Labelled test chemical

Phenanthrene, a three ringed hydrocarbon, is one of the most abundant PAHs present in coastal oceanic waters (Mojiri et al., 2019) and is often studied as a model oil-derived pollutant (Cennerazzo et al., 2017; Chen et al., 2018; Echeveste et al., 2010). Stable carbon isotope-labelled phenanthrene ($^{13}C_{14}H_{10}$, molecular weight 192.13 g/mol) with 99 atom% purity was purchased from Sigma-Aldrich Chemie GmbH (Product number: 703,125, CAS number: 1262770-68-2). Working solutions of ^{13}C-phenanthrene were prepared in HPLC-grade methanol (Sigma-Aldrich) in amber glass GC-vials with Teflon™-lined screw caps. Aqueous test solutions were sonicated to promote dissolution before use.

2.2. CRDS instrumentation and analytical method

Accumulation of ^{13}C-phenanthrene in coral tissues and phytoplankton cultures was calculated from analysis of carbon content and isotopic composition with a combustion module (Costech Analytical Technologies Inc., California, USA) attached to a CRDS system (CM-CRDS G2201-I, Picarro Inc, Santa Clara CA, USA). CRDS is a highly sensitive technique resulting from long absorption path lengths (i.e., 20–25 km effective path length, G2201-i, Picarro system) that allows detection of absolute concentration of ^{13}C-labelled compounds in small samples, while simultaneously measuring the total organic carbon content (Graham et al., 2010). Coral tissue and phytoplankton samples were collected on glass fibre filters (25 mm diameter, Whatman™), dried and cut in half. Each half was packed in an individual tin capsule (10×13 mm). The tin-capsules were loaded in an auto-sampler supplying to a combustion quartz tube (prepacked reaction tube, SW, Picarro, CM 61134, OEA Labs) surrounded by a furnace maintained at 980 °C. Combustion of samples raised the temperature to between 1700 °C and 1800 °C for a few seconds. The CO_2 produced during combustion was pumped into the isotopic analyser to measure the total carbon content and delta per mil ($\delta^{13}C$ ‰) value. Since isotopic differences between substances can be exceedingly small (Sulzmann, 2007), the $\delta^{13}C$ ‰ value is used to express isotopic composition of any measured substance relative to a recognized standard. The universal standard for carbon isotopes is Vienna Pee Dee Belemnite.

The CRDS was calibrated by running internal standards with a range of $\delta^{13}C$ ‰ values, prior to samples. Internal standards used ranged from -3.22 $\delta^{13}C$ ‰ (sodium bicarbonate) to -31.1 $\delta^{13}C$ ‰ (phthalic acid). Accuracy of the Picarro-CRDS method, estimated as the difference between certified $\delta^{13}C$ ‰ value and the measured $\delta^{13}C$ ‰ value of a standard, ranged from -0.19 ± 0.07 to 2.22 ± 0.12 $\delta^{13}C$ ‰. The overall percentage recovery of known $\delta^{13}C$‰ values of the standards was 95.67 ± 14.61% (mean ± standard error (SE)) for 92 internal standard measurements. The unknown carbon concentration of sample filters was calculated using a calibration curve prepared using a standard with known $\delta^{13}C$ ‰ value and carbon content. Calibration curves were made over a concentration range from 80 to 1000 μg C.

2.3. Dunaliella salina cultures – ^{13}C- phenanthrene accumulation and exposure effects

2.3.1. Experiment setup and sampling

Cultures of the marine microalga *Dunaliella salina* CS265 (Australian National Algae Supply Service, CSIRO Hobart, Australia) were grown in 0.2 μm filtered seawater f/2 culture medium. Accumulation and effect of ^{13}C-phenanthrene was tested by exposing *D. salina* to a gradient of increasing phenanthrene concentrations of 1, 3, 10, 30, 100, 300 and 900 μg L^{-1} for 48 hours in 250 mL capacity Erlenmeyer flasks, in triplicate with a test volume of 100 mL. The test flasks were kept at 26 ± 0.5 °C, under an irradiation of 130 ± 10 μmol photons m^{-2} s^{-1} and 12:12 light: dark cycle with gentle shaking at 80 rpm in a temperature-controlled, shaking incubator (Model: TLM-520, Thermoline Scientific). The solvent concentration in the test was 0.05% v/v. Triplicate flasks without ^{13}C-phenanthrene and flasks spiked with only methanol (HPLC grade) at 0.05% were run as controls and solvent controls respectively. At the start, and after 24 and 48 hours of exposure, the cell abundance and photosynthetic parameters were measured by flow cytometry and pulse-amplitude-modulation (PAM) fluorometry, respectively, as described in later sections. After 48 hours, remaining algal culture in each flask (> 90 mL) was filtered through pre-combusted glass fiber filters (25 mm diameter, GF/F, Whatman™) retaining the algal biomass. The filters were treated to concentrated hydrochloric acid (HCl) fumes in a chamber overnight to remove all inorganic carbon, placed in a desiccator, and stored frozen at −20 °C. Filters were later analyzed for $\delta^{13}C$ ‰ and carbon content in Picarro CRDS.

2.3.2. Estimation of D. salina cell abundance and lethal concentration (LC) values

D. salina cell abundance was measured with BD Accuri™ C6 Plus bench-top flow cytometer providing absolute counts with inbuilt BD Accuri™ C6 Plus software. A fresh sample (1 mL) from each flask was individually loaded using SIP (sample injection port) tubes (SARSTEDT,

Germany). 100 μL of the culture was counted at a speed of 5 μL s^{-1}. Data were acquired in log mode with a range of 10^1 to 10^7 decades. The population was identified and gated on FSC (forward scatter) vs. SSC (side scatter), and FL-3 (red fluorescence; chlorophyll) vs. FL-2 (orange fluorescence; carotenoids) dot plots. The FL-3 vs. FL-2 gate was used to measure cell abundance. Effect of exposure of ^{13}C-phenanthrene to D. salina was quantified as the lethal concentrations leading to 25% and 50% decline in population abundance (LC_{25} and LC_{50}, respectively) measured via flow cytometry. LC values were calculated from the slope of the relationship between initial dosages and the decline in cell abundance at 48 hours of exposure, as described in (Echeveste et al., 2010).

2.4. Coral ^{13}C-phenanthrene uptake and exposure effects

2.4.1. Experimental setup for coral uptake

Acropora millepora colonies used in the experiments were collected from ~5 m depth at Trunk Reef (S 18°18.101′, E 146°52.226'), Great Barrier Reef (GBR), fragmented to ~2 cm length, healed and acclimatized in flow-through seawater systems for over a fortnight at the National Sea Simulator (SeaSim), Australian Institute of Marine Science, Townsville. Three colonies were sampled for this experiment. Seawater used in the treatments was pumped from offshore, pre-filtered through the SeaSim Seawater Treatment System, and filtered again with 0.2 μm filter prior to use in the experiments. In the experiment, *A. millepora* fragments were exposed to ^{13}C-phenanthrene at two concentration levels via either addition of labelled *D. salina* cells in seawater **(dietary exposure treatments)** or ^{13}C-phenanthrene dissolved directly in seawater **(aqueous exposure treatments).** The microalga, *D. salina* was selected as the labelled food source after microscopic monitoring of polyp behavior. *D. salina* is also regularly used in live feed mix for corals maintained in SeaSim. Each treatment consisted of 6 replicated jars with 3 coral fragments in each jar containing 150 mL seawater. Fragments were so distributed to have one from each of three *A. millepora* colonies in each jar. Phenanthrene concentrations used in this study were selected to achieve a balance between sufficient signal detection in the CRDS, toxicity and solubility in seawater. *D. salina* cultures were labelled at LC_{25} (182 μg L^{-1}) and LC_{50} (440 μg L^{-1}) concentrations in seawater f/2 culture medium for 48 hours, and counted in the flow cytometer at 0 and 48 hours. For dietary exposure, corals were provided D. salina at 10% of the total test volume, by adding 15 mL of labelled *D. salina* culture to the respective treatment jars. Cell concentrations of *D. salina* in the coral treatment jars were maintained $3 \times 10^4 \pm 4.5 \times 10^3$ cells mL^{-1}. The final exposure concentrations of ^{13}C-phenanthrene to the corals were 18.2 and 44 μg L^{-1}. For aqueous treatments, ^{13}C-phenanthrene was directly dissolved in seawater to achieve the same concentrations as those in the dietary exposure. In total, we tested four treatments combining two exposure routes (dietary, aqueous) and two ^{13}C-phenanthrene concentrations (18.2 and 44 μg L^{-1}). Controls for dietary and aqueous treatments were corals maintained in plain seawater, with and without the addition of unlabelled *D. salina*, respectively. The experiment was maintained for six days with a daily renewal of the seawater medium. Coral health was monitored by measuring the photosystem health and bleaching stress index as described in later sections.

2.4.2. Sampling and analysis of coral fragments

Six coral fragments were sampled, collected as one per jar, on days 2, 4 and 6 from each treatment. Sampled fragments were quickly wrapped in aluminum foil, frozen immediately and stored at −20 °C until analysis. Frozen coral fragments were airbrushed with 5 mL of MilliQ water to remove all tissue. 1 mL of 10% HCl was added to the tissue slurry and placed in an acid fume chamber to remove all inorganic carbon. The tissue was then filtered onto pre-combusted filters (25 mm diameter, GF/C, Whatman™), dried, and placed in a desiccator before packing in tin-capsules. Filters that were not immediately analyzed were kept frozen at −80 °C. The δ^{13}C ‰ and carbon content were analyzed from dried filters following the CRDS analytical method described above.

2.4.3. Monitoring of treatment water quality

Water quality parameters were measured in coral treatment jars (up to 6 jars chosen at random on each day) using dissolved oxygen (HQ30d equipped with an Intellical LDO101 oxygen probe (Hach, USA)), pH, temperature and salinity probes (Horiba LAQUAact PC110). Measurements remained stable through the experiment, with pH 8.10 ± 0.004, dissolved oxygen 8 ± 0.02 mg O_2 L^{-1}, salinity 35.1 ± 0.03 g L^{-1} and water temperature of 24.4 ± 0.09 °C.

2.4.4. Coral health index

Coral health was also monitored by visually comparing high-resolution digital photographs of the fragments from all treatments and controls with the coral health index card to observe for bleaching distress (Siebeck et al., 2006).

2.5. Photophysiology of corals and microalgae

The photophysiological response of microalgae and corals to the experimental conditions was measured by PAM fluorometry (Maxi-Imaging-PAM, Heinz Walz, GmbH, Germany). This non-invasive technique is valuable for assessing the function of Photosystem II (PSII) by measuring the maximum quantum yield (F_v/F_m), a measure of photosynthetic efficiency (Ralph et al., 2007). Photophysiological responses of *D. salina* and corals were analyzed by measuring minimal (F_0) and maximal fluorescence (F_m), from which F_v/F_m was calculated as the ratio of variable to maximum fluorescence ($F_v/F_m = (F_m - F_0)/F_m$). Briefly, *D. salina* culture samples from different treatments were aliquoted into 48 well plates. Coral fragments were individually placed in glass trays filled with filtered seawater. All samples were incubated in darkness for 15 min before analyses. Dark-adaptation of samples opens maximum PSII reaction centers and results in a minimal level of initial F_0 (Ralph et al., 2007). Instrument settings were optimized (measuring light (ML) intensity 3 and ML pulse frequency 8, corresponding to an integrated photosynthetically active radiation photon flux density of 1 μmol m^{-2} s^{-1}) to measure F_0 of the dark-adapted sample and F_m on a saturation pulse (Schreiber et al., 2007).

2.6. Calculation of ^{13}C-phenanthrene accumulation and BCF

Previously, calculation of photosynthesis rates based on stable isotopic tracer incorporation have been described (López-Sandoval et al., 2019). Here, from δ^{13}C ‰ values and carbon content of the samples, we describe calculation of accumulated ^{13}C-phenanthrene concentrations in microalgae cells, and coral tissue. The δ^{13}C ‰ value expresses the δ^{13}C ratio of the sample relative to an internationally accepted standard in parts per thousand deviation from that standard by:

$$\delta‰ = \left(\frac{R_{sample}}{R_{standard}} - 1\right) \times 1000 \quad (1)$$

where.

R is typically the ratio of rare-to-abundant isotope, and R_{sample} and $R_{standard}$ are the ratios of sample and universal standard, respectively. The isotopic ratio of Vienna Pee Dee Belemnite is 0.0112372. From the δ^{13}C ‰ value of the samples and controls, we calculated their respective R values. The R value was then converted to the fractional abundance of ^{13}C (F) by,

$$F = R/(1 + R) \quad (2)$$

Fractional abundance of excess ^{13}C above the natural isotopic signature (of controls) was calculated as:

$$F_{excess} = F_{sample} - F_{control} \quad (3)$$

Table 1
Physiological effects, changes in $\delta^{13}C‰$ values and cellular accumulation of ^{13}C-phenanthrene in D. salina after 48-h exposure to a range of 0–900 μg L^{-1}. All parameters reported are mean ± SE.

Nominal concentration of ^{13}C-phenanthrene (μg L^{-1}) in seawater	Cell abundance (cells mL^{-1})	Specific growth rate (divisions day^{-1})	$\delta^{13}C$ ‰	^{13}C-phenanthrene accumulated (fg $cell^{-1}$)	Residual concentration of ^{13}C-phenanthrene (μg L^{-1}) in seawater
0	6.10 E+05 ± 1.97 E+04	0.95 ± 0.02	−23.46 ± 0.04	–	–
1	5.95 E+05 ± 3.21 E+04	0.94 ± 0.03	−14.33 ± 0.04	2.37 ± 0.24	0.60 ± 0.06
3	6.34 E+05 ± 2.05 E+04	0.97 ± 0.01	−10.94 ± 0.12	3.09 ± 0.06	1.80 ± 0.06
10	5.81 E+05 ± 6.34 E+03	0.93 ± 0.00	0.99 ± 0.52	6.63 ± 0.32	6.17 ± 0.18
30	5.97 E+05 ± 1.26 E+04	0.94 ± 0.01	33.34 ± 1.19	15.20 ± 0.67	15.67 ± 0.67
100	5.04 E+05 ± 8.52 E+03	0.86 ± 0.01	149.53 ± 3.77	56.66 ± 3.22	49.00 ± 3.21
300	4.16 E+05 ± 1.72 E+04	0.76 ± 0.02	386.79 ± 18.46	104.85 ± 5.64	96.67 ± 9.40
900	1.43 E+05 ± 2.33 E+03	0.23 ± 0.01	4664.32 ± 366.35	1546.69 ± 366.14	211.67 ± 8.99

where.

$F_{control}$ is the fractional abundance in natural control samples and F_{sample} is the fractional abundance of samples exposed to ^{13}C-phenanthrene.

The mass of carbon (g) measured per sample was converted to moles by dividing by the molecular mass of carbon. Total moles carbon was multiplied by F_{excess} to provide the moles of $^{13}C_{excess}$.

$$\text{Moles}^{13}C_{excess} = \text{mass of carbon(g)}/12 * F_{excess} \quad (4)$$

Finally, the quantity of ^{13}C-phenanthrene accumulated was calculated as

$$\textit{phenanthrene accumulated}\ (g) = (\text{moles}^{13}C_{excess}/14) * 192.13\ g\ \text{mol}^{-1} \quad (5)$$

where.

14 is the number of moles of ^{13}C in 1 mole of phenanthrene, and 192.13 is the molecular weight of ^{13}C-phenanthrene.

The calculated quantity of ^{13}C-phenanthrene (g) in *D. salina* cultures was, dividing by the respective cell abundances, converted to femtograms (fg $cell^{-1}$). Phenanthrene accumulated in coral biomass was calculated as μg per fragment and normalized to the coral surface area (μg cm^{-2}). The surface area of *A. millepora* fragments (n = 78) with an average length of 1.8 ± 0.018 cm (mean ± SE), was calculated using simple geometry, approximating it to a cylinder according to (Naumann et al., 2009). Briefly, the total height, maximum and minimum diameters of each individual fragment was measured using Vernier calipers. Surface area of the cylinder was calculated applying formula ($2\ \pi\ r\ h + (2\ \pi\ r^2)$).

The bioconcentration factor BCF (L Kg^{-1}, dry weight) was calculated as the ratio of the ^{13}C-phenanthrene concentration in the organism (C_{org}) relative to the concentration in water (C_w):

$$BCF = \frac{Corg}{Cw} \quad (6)$$

Dry weight of *D. salina* was derived from the cell volume (Reynolds, 1984). Dry weight of coral tissue biomass was obtained from the difference in dry weight of filter before and after filtration. Tissue dry weight of the *A. millepora* fragments was 4.70 ± 0.76 mg (n = 8, mean ± SE). The uptake rate (μg cm^{-2} day^{-1}) of ^{13}C-phenanthrene in coral was calculated as the slope of the relationship between quantity of ^{13}C-phenanthrene accumulated in coral versus time.

2.7. Analysis of residual ^{13}C-phenanthrene concentration in seawater by GC-MS/MS

The residual concentration (μg L^{-1}) of ^{13}C-phenanthrene in seawater was analyzed by gas chromatography tandem mass spectrometry (GC-MS/MS) following solid-phase extraction (SPE). Residual seawater concentrations measured here could reflect fractions that were both freely dissolved and bound to organic carbon. Between 90 and 100 mL of water samples from the experiments were collected in 125 mL amber glass bottles with Teflon™-lined screw-caps, noting the volume. Seawater samples from the *D. salina* accumulation and toxicity test were collected at the end of 48 hours after filtration retaining the algal biomass. From the coral experiment, seawater was collected without filtration after 24 hours of exposure and directly transferred to amber glass bottles. Water samples from the coral experiment were collected only on Day 6 of exposure. All samples were acidified to pH 2 using HCl and stored frozen at −20 °C until analysis. For extraction of samples, SPE cartridges (Chromabond® C18 (500 mg/3 mL) from Macherey-Nagel) were conditioned with 6 mL of methanol and 6 mL of MilliQ water. Then, 10 mL of sample was loaded and consequently, the SPE cartridges were dried under vacuum. The elution of ^{13}C -phenanthrene was carried out with 5 mL of dichloromethane. The extracts were concentrated to dryness using Rocket™ Evaporation system and then reconstituted with 0.9 mL of dichloromethane and 0.1 mL of internal standard (phenanthrene-d_{10} at 1000 μg L^{-1}).

One microliter of extract was injected in splitless mode in a GC-MS/MS instrument (Agilent 7890 GC 7010B/MS Triple Quadrupole mass spectrometer) using a HP-5MS, 30 m length, 0.25 mm inner diameter and 0.25 μm film thickness capillary column. The injector temperature was 310 °C. The temperature program of the oven was as follows: 80 °C maintained for 1 min, then raised at 25 °C min^{-1} up to 200 °C, raised at 10 °C min^{-1} up to 335 °C and maintained for 6.3 min. Helium at 1.1 mL min^{-1} in constant flow was used as the carrier gas. Backflush of helium at 1.5 mL min^{-1} for 3 min was used to clean up the column after each injection. The temperature of the interface was maintained at 320 °C. The mass spectrometer was operated in multiple reaction mode (MRM). Nitrogen at 1.5 mTorr was used as the collision gas. The monitored transitions for ^{13}C-phenanthrene were 192.5 > 190.1 (collision energy CE 35.0 V) and 192.5 > 164.1 (CE 35.0 V), and for phenanthrene-d_{10} 188.3 > 186.3 (CE 15.0 V) and 188.3 > 160.2 (CE 20.0 V). ^{13}C-phenanthrene was quantified by an external calibration curve of ^{13}C-phenanthrene with concentrations from 1 to 100 μg L^{-1} in dichloromethane. All standards contained phenanthrene-d_{10} at 100 μg L^{-1} as an internal standard. The identity of ^{13}C-phenanthrene was confirmed by the similarity of retention times and ion ratios between the sample extract and the standards. Practical quantitation limit (PQL) of the method was 0.1 μg L^{-1}. Blank samples spiked at 5 μg L^{-1} were included in every batch of analysis as quality control samples. Recoveries of nominal concentration of spiked samples ranged from 76 to 91%.

2.8. Data analysis

Data were analyzed in JMP Pro software (version 13.1, SAS Institute, USA), and plots were made using Origin Pro V 8.0 (Origin Lab Corporation, USA). The data obtained were analyzed by independent *t*-test and one-way analysis of variance (ANOVA). The treatment means for *D. salina* F_v/F_m were compared by Tukey's post hoc multiple comparison test. Individual tests conducted are described with each result.

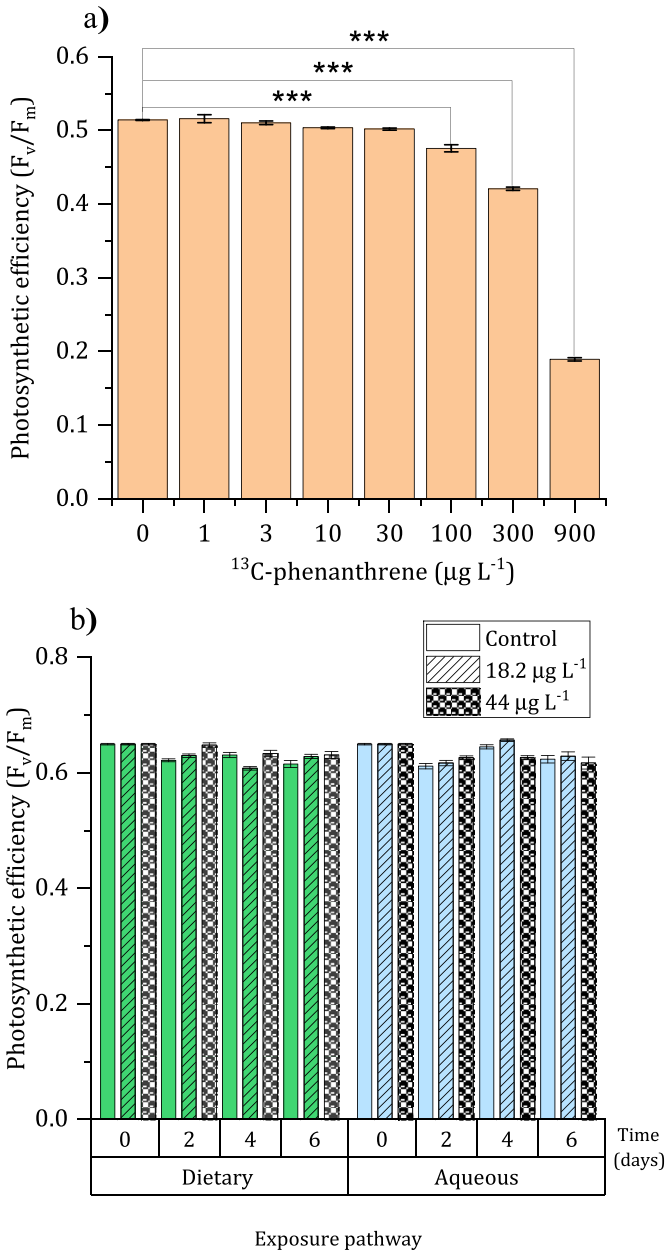

Fig. 1. Changes in photosynthetic efficiency (F_v/F_m) (mean ± SE) of *D. salina* cultures and coral fragments observed in controls and when exposed to ^{13}C-phenanthrene. **(a)** Bar graph showing decline in F_v/F_m in *D. salina* cultures exposed to a range of ^{13}C-phenanthrene concentrations. **(b)** Grouped bar plot of F_v/F_m in *A. millepora* fragments exposed to ^{13}C-phenanthrene via dietary (green bars) and aqueous (blue bars) exposure pathways. Bars marked by *** show < 0.001 significant difference from all other treatment concentrations at 0.05 level analyzed by one-way ANOVA and Tukey's posthoc test for pair-wise differences. (For interpretation of the references to color in this figure legend, the reader is referred to the Web version of this article.)

3. Results

3.1. Effects of phenanthrene exposure in D. salina

Exposure to ^{13}C-phenanthrene reduced the cell abundance and photosynthetic efficiency in *D. salina* cultures, particularly at higher concentrations. Exposure to the highest concentration of ^{13}C-phenanthrene (900 µg L^{-1}) used in the toxicity test, resulted in a ~76% reduction in cell abundance and specific growth rate of *D. salina* (Table 1). Moreover, F_v/F_m of *D. salina* was significantly affected ($p < 0.05$) at all concentrations above 100 µg L^{-1} (Fig. 1a). The LC_{25} and LC_{50} concentrations obtained for *D. salina* were 182 µg L^{-1} and 440 µg L^{-1} of ^{13}C-phenanthrene respectively, and were used to label the *D. salina* cells in subsequent coral exposure experiments.

3.2. Accumulation of ^{13}C-phenanthrene in D. salina

D. salina cells were gradually enriched in ^{13}C with increasing doses of ^{13}C-phenanthrene, altering the δ^{13}C signal after 48 hours of exposure (Table 1). Isotopic composition values reflecting the cellular accumulation of ^{13}C-phenanthrene significantly increased from −23.46 ± 0.04 δ^{13}C ‰ , the value determined to represent the natural isotopic ratio in the *D. salina* cells in culture conditions, to 4664 ± 366 δ^{13}C ‰ , at 900 µg L^{-1} of ^{13}C-phenanthrene (Table 1). The analytical precision of the Picarro-CRDS method (determined as the standard error of the mean from 8 replicated samples) was ± 0.041‰ for algal δ^{13}C with detection of accumulation of ^{13}C from labelled phenanthrene even at the lowest concentrations tested (1 µg L^{-1}, Table 1). The calculated amount of ^{13}C-phenanthrene accumulated in *D. salina* (y) ranged from 2.37 ± 0.24 fg cell^{-1} to 1547 ± 366 fg cell^{-1} (Table 1), increasing linearly ($y = 0.892x + 0.076$, $R^2 = 0.92$, $p = < 0.0001$) with increasing ^{13}C-phenanthrene dosage (Fig. 2a). The residual ^{13}C-phenanthrene concentration in seawater after *D. salina* uptake indicated that more than 50% of the phenanthrene was absorbed by the cells (Table 1). The mean BCF of ^{13}C-phenanthrene in *D. salina* per dry weight was 2590 ± 787 L kg^{-1} (log BCF = 3.41).

3.3. Effect of ^{13}C-phenanthrene exposure on coral health

The ^{13}C-phenanthrene exposure and absorption/uptake at two tested concentrations (18.2 µg L^{-1} and 44 µg L^{-1}) had no detectable adverse effects on photophysiology of *A. millepora*, as shown by the insignificant differences in F_v/F_m (F-ratio = 1.1985; DF = 142; p = 0.2755, one-way ANOVA) between the control and treated coral fragments (Fig. 1b). Through the experiment, the corals exhibited visibly normal polyp extension. We also observed no visual signs of bleaching by comparing images of coral fragments taken on each sampling day with the coral health color index charts (Fig. 3).

3.4. Accumulation of ^{13}C-phenanthrene by corals via seawater and dietary exposure routes

3.4.1. Enrichment of heavy isotope (^{13}C) in coral tissues

Across all treatments, *A. millepora* exposed to ^{13}C-phenanthrene showed significant enrichment in the heavy isotope, ^{13}C, with more positive δ^{13}C‰ values than the natural isotopic composition of coral tissues (−17.17 ± 0.10 δ^{13}C‰; mean ± SE) (Table 2). The analytical precision of the Picarro-CRDS method for corals was ± 0.051 mg C for coral fragments (determined as the standard error of the mean from 8 replicated samples). All treatments showed increasingly positive δ^{13}C‰, values with increasing exposure time, demonstrating that coral fragments accumulated ^{13}C-labelled phenanthrene directly from seawater as well as from labelled *D. salina* (Table 2). Irrespective of the exposure pathway, there was a greater enrichment of ^{13}C in tissues of corals exposed to 44 µg L^{-1} equivalent treatments in comparison with the lower 18.2 µg L^{-1} equivalent treatments at all time points (Fig. 2b and c). The residual ^{13}C-phenanthrene concentration in water after 24 hours exposure was lower than the initial concentration added, with small differences between treatments (Table 2), over all indicating that corals could absorb up to 70% of the initial phenanthrene present in seawater.

3.4.2. Coral uptake rates, accumulation and BCFs

Comparing the ^{13}C-phenanthrene accumulation over time, we found that the uptake rate by corals via aqueous exposure was twice that of exposure to labelled *D. salina* in dietary treatments (t-value = 74.46;

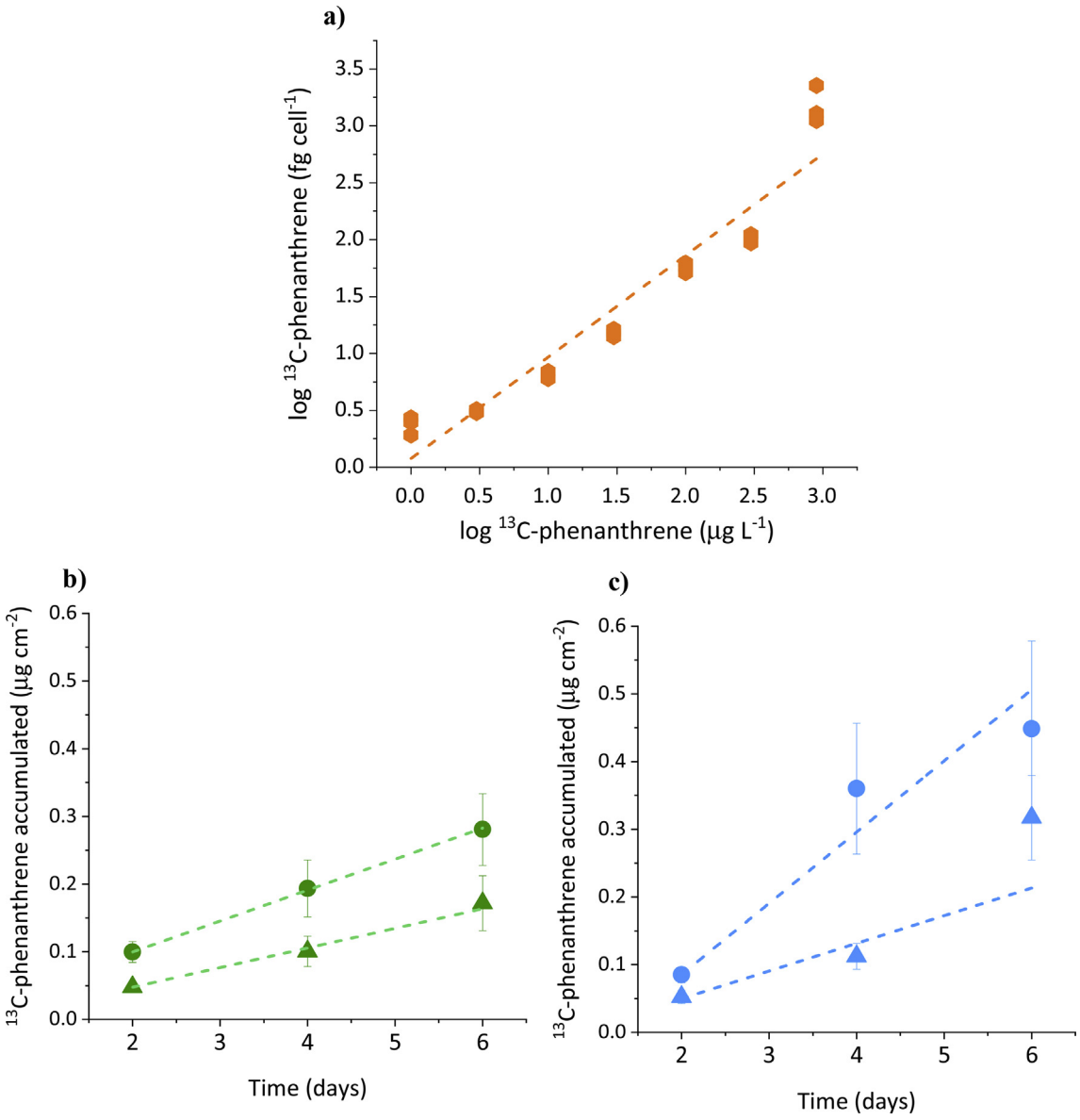

Fig. 2. Accumulation of ^{13}C-phenanthrene in microalgae and corals. **(a)** Fitted linear regression showing the relationship between accumulation of ^{13}C-phenanthrene in *D. salina* cells (fg cell^{-1}) and ^{13}C-phenanthrene concentration in seawater (µg L^{-1}). Uptake of ^{13}C-phenanthrene by *A. millepora* fragments, as mean ± SE accumulated ^{13}C-phenanthrene (µg cm^{-2}) over time (days), through **(b)** dietary exposure (via labelled *D. salina*) and **(c)** aqueous exposure, at the nominal phenanthrene concentrations of 18.2 µg L^{-1} (triangles ▲, ▲) and 44 µg L^{-1} (circles ●, ●). Lines represent the linear fitted regression.

DF = 70; p < 0.0001, *t*-test) (Table 2; Fig. 2b and c). However, we found no significant differences in total ^{13}C-phenanthrene accumulated into coral tissues between dietary treatments containing labelled *D. salina* and aqueous treatments exposing corals purely via passive diffusion (F-ratio = 3.7266, p = 0.0576; DF = 70, one-way ANOVA) (Fig. 4). Moreover, the distribution of δ^{13}C‰ values, and consequently, accumulation across replicates was narrower in dietary treatments, compared to that in aqueous treatments (Fig. 4). The variability observed between replicates was above the analytical precision obtained with the Picarro-CRDS method (± 0.1‰ and ± 0.1 mg C for the coral tissues). Coral BCF estimated was 5266 ± 812 L kg^{-1} (log BCF = 3.72) for aqueous exposure route and 3779 ± 532 L kg^{-1} (log BCF = 3.58) for dietary exposure route. A steady-state in terms of body burden was not reached in this experiment.

4. Discussion

Accumulation in phytoplankton can control the aquatic fate of hydrophobic organic pollutants such as PAHs, and this represents an important pathway for their incorporation into marine food-chains (Fan and Reinfelder, 2003; Koelmans, 2014; Spann et al., 2015). Previously, studies have shown incorporation of algal carbon into marine copepods and deep-sea foraminifera via uptake of stable isotope labelled $NaH^{13}CO_3$ (Graeve et al., 2005; Nomaki et al., 2005), which is an excellent source of carbon for autotrophs (López-Sandoval et al., 2019). Here, combining ^{13}C-labelling and CRDS, we demonstrated the accumulation of the model PAH ^{13}C-phenanthrene in *D. salina*, a marine microalgae and followed its transfer into the coral, *A. millepora*. While use of stable-isotopic carbon labelling effectively eliminates radioactive toxicity risks associated with radioactive tracers (Limer et al., 2015) which have so far been commonly used (Fan and Reinfelder, 2003; Jensen et al., 2012), its application in combination with the CRDS analytical method also reduces the need for conventional high-cost instrumentation such as GC-IRMS requiring greater sample volume and elaborate preparation steps such as pressurized solvent extraction, purification, concentration *et cetera* (Martinez et al., 2004; Wan et al.,

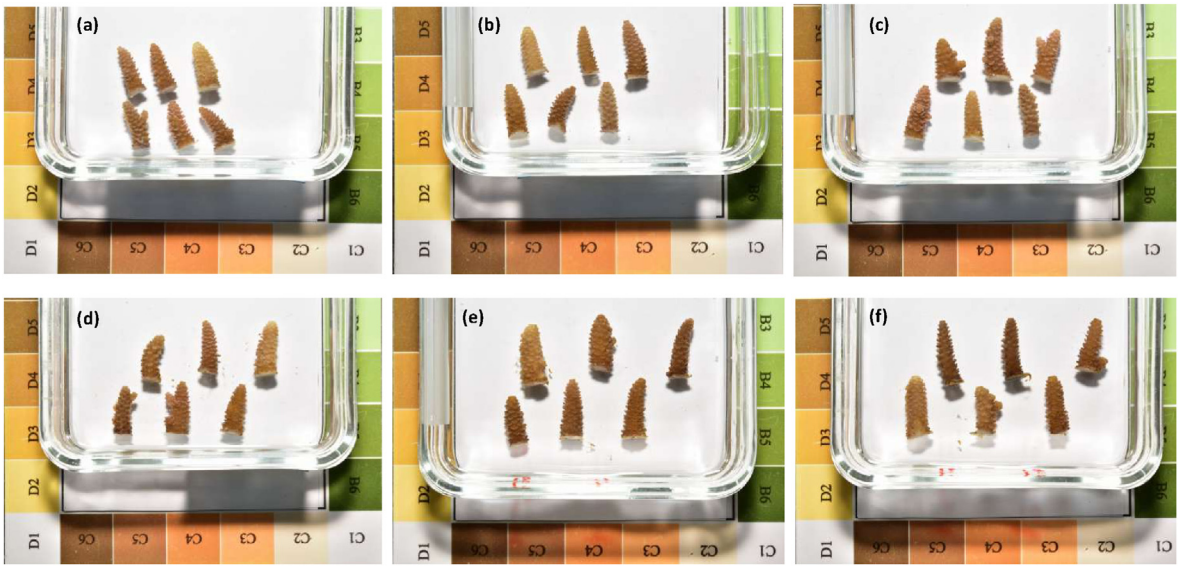

Fig. 3. *A. millepora* replicate fragments with the coral health chart on Day 6 of the experiment. (a) Control (b) Aqueous exposure at 18.2 μg L^{-1} (c) Aqueous exposure at 44 μg L^{-1} (d) Control fed unlabelled *D. salina* (e) Dietary exposure at 18.2 μg L^{-1} (f) Dietary exposure at 44 μg L^{-1}.

2007). Further, tracking the transfer of metabolites which are challenging to resolve and quantify (Carrasco Navarro et al., 2013), is also solved by tracing the total accumulation of ^{13}C.

The accumulated concentrations of ^{13}C-phenanthrene per cell (fg $cell^{-1}$) in *D. salina* (Table 1, Fig. 1) were close to those reported by Fan and Reinfelder (2003) for marine diatoms using ^{14}C-phenanthrene under similar feeding densities. In that study, *Thalassiosira weissflogii* and *Thalassiosira pseudonana* accumulated about 90 and 4.5 fg $cell^{-1}$, after two days of exposure to about 16 and 14 μg L^{-1} of ^{14}C-phenanthrene respectively (Fan and Reinfelder, 2003). The large range in accumulated concentration could be due to inter-specific variations in size, surface properties and cell wall characteristics (Fan and Reinfelder, 2003; Plant et al., 1987). High concentrations of phenanthrene can be acutely toxic to phytoplankton (Chen et al., 2018; Echeveste et al., 2010). Cultures of *D. salina* exposed to ^{13}C-phenanthrene exhibited sub-lethal toxicity at higher concentrations (> 100 μg L^{-1}); toxicity thresholds that caused 25 and 50% acute decline in D. salina cell abundance in this study are similar to that reported for *Chlorella salina* (Chen et al., 2018), and substantially higher than those for smaller phytoplankton species (Echeveste et al., 2010). In addition to inhibition of growth, ^{13}C-phenanthrene also caused damage to PSII as shown by the decrease in F_v/F_m. The decline in photosynthetic efficiency was similar to that of growth, but inhibition by ^{13}C-phenanthrene was not as great as for PSII herbicides such as diuron which exhibit an EC_{50} in the low μg L^{-1} range (Mercurio et al., 2018).

Sorption of pollutants by microalgae is highly relevant, considering their large surface area for uptake from seawater (Gerofke et al., 2005; Koelmans, 2014; Mallhot, 1987). The BCF of phenanthrene in *D. salina* (log BCF = 3.41) calculated using this ^{13}C-labelling method was close those values reported for phytoplankton reported using radioactive labelled organic chemicals (Freitag et al., 1985), and within the range of ^{14}C-phenanthrene log BCF reported in other studies: 3.2 for *Chlorella fusca* (Geyer et al., 1991) to 4.03 for *Selenastrum capricornutum* (Casserly et al., 1983; Halling-Sørensen et al., 2000). The reported BCF represents a realistic pathway for incorporation into phytoplankton potentiating trophic transfer of phenanthrene.

The natural carbon isotopic composition of *A. millepora* measured here using CRDS (−17.17 ± 0.10 $\delta^{13}C$‰; mean ± SE) is within the range of $\delta^{13}C$‰ reported for symbiotic coral tissue (−12.8 $\delta^{13}C$‰ to −20.8 $\delta^{13}C$‰) (Muscatine et al., 2005). Scleractinian corals are known as predatory and suspension feeders (Anthony, 1999; Towle et al., 2015), in addition to the utilization of photosynthates produced by endosymbiotic algae (Tremblay et al., 2012). While consortia of phytoplankton are major components of suspended particulate matter that corals feed on (Anthony, 2000, 1999), species specific herbivory is also reported in corals (Houlbrèque et al., 2004; Leal et al., 2014; Osinga et al., 2012; Piccinetti et al., 2016). Phytoplankton concentrations we used in the dietary exposure treatments are similar to those used with mussels in the presence of algal feed to test the accumulation of phenanthrene (Yakan et al., 2013) and within feeding rates estimated for corals (Orejas et al., 2016). The estimated carbon content (μg C L^{-1}) introduced by an addition of *D. salina* (21.6 ± 0.8 pgC $cell^{-1}$) at an average concentration of 3.00 E+04 cells mL^{-1} in dietary exposure treatments was 648 μg C L^{-1}. The GBR waters previously characterized by low carbon concentrations between 0.95 and 21.6 μg C L^{-1} (Ayukai, 1995), have in recent times shown steep increases with values ranging from 788 to 1398 μg C L^{-1} (Schaffelke et al., 2011).

Uptake kinetics of PAHs in marine organisms has been quantified previously using ^{14}C-phenanthrene, however, most studies used aqueous rather than dietary exposure (Bustamante et al., 2012; Jensen et al., 2012; Solbakken et al., 1984; Valdez Domingos et al., 2011). Even so, estimates of uptake rates of PAHs in corals are scarce in literature; Kennedy et al. estimated uptake rate of benzo(a)pyrene (BaP) as 6.5 ± 0.7 and 10.8 ± 0.2 μg BaP cm^{-2} h^{-1} for the corals, *Favia fragrum* and *Montastrea annularis*, via diffusive processes alone. Higher uptake rates for BaP compared to phenanthrene could be due to the greater affinity of BaP to tissue lipids and inter-specific differences in coral surface morphology (Kennedy et al., 1992). Existing studies on corals have only investigated aqueous uptake and depuration (Kennedy et al., 1992; Knap et al., 1982; Solbakken et al., 1984)). Our study provides the first evidence for uptake of ^{13}C-labelled phenanthrene in coral tissue via contaminated microalgae, comparing it with purely diffusive uptake from seawater.

Some studies with other aquatic organisms have compared the uptake rates and accumulation of PAHs through different exposure routes (Arias et al., 2016; Berrojalbiz et al., 2009; Lu et al., 2004). For instance, Spann et al. compared ^{14}C-phenanthrene uptake in nematodes in the presence and absence of bacterial food and reported that the dissolved phase phenanthrene contributed most to the accumulated body burdens, even in the presence of food with an average uptake rate of 244 ± 26 L Kg_{nem}^{-1} h^{-1} (Spann et al., 2015). However, they reported substantially higher tissue concentrations after 24 hours, elevated toxicity and lower growth in nematodes exposed via dietary uptake (Spann et al., 2015). This finding is also supported by previous

Table 2
Carbon isotopic composition ($\delta^{13}C$ ‰), accumulation and uptake rate of ^{13}C-phenanthrene in *A. millepora* tissue in dietary and aqueous treatments. *Significantly different. t-value = 74.46; DF = 70; p < 0.0001.

Nominal ^{13}C-phenanthrene concentration →		18.2 µg L^{-1}				44 µg L^{-1}			
Treatment	Days	$\delta^{13}C$ ‰	^{13}C-phenanthrene accumulated (µg cm^{-2})	Uptake rate (µg cm^{-2} day^{-1})	Residual ^{13}C-phenanthrene concentration (µg L^{-1})	$\delta^{13}C$ ‰	^{13}C-phenanthrene accumulated (µg cm^{-2})	Uptake rate (µg cm^{-2} day^{-1})	Residual ^{13}C-phenanthrene concentration (µg L^{-1})
Dietary exposure	2	−8.72 ± 0.35	0.048 ± 0.006	0.03 ± 0.004	5.48 ± 0.29	9.53 ± 5.92	0.100 ± 0.015	0.045 ± 0.009	11.88 ± 0.42
	4	3.48 ± 2.05	0.101 ± 0.023			25.36 ± 8.42	0.194 ± 0.042		
	6	9.40 ± 3.62	0.172 ± 0.041			42.94 ± 7.10	0.281 ± 0.053		
Aqueous exposure	2	−7.81 ± 0.84	0.052 ± 0.010	0.06 ± 0.009*	5.31 ± 0.22	3.40 ± 2.60	0.085 ± 0.012	0.09 ± 0.05*	14.81 ± 0.69
	4	4.07 ± 1.03	0.112 ± 0.019			32.46 ± 5.91	0.360 ± 0.097		
	6	23.71 ± 3.69	0.317 ± 0.062			51.88 ± 14.49	0.448 ± 0.130		

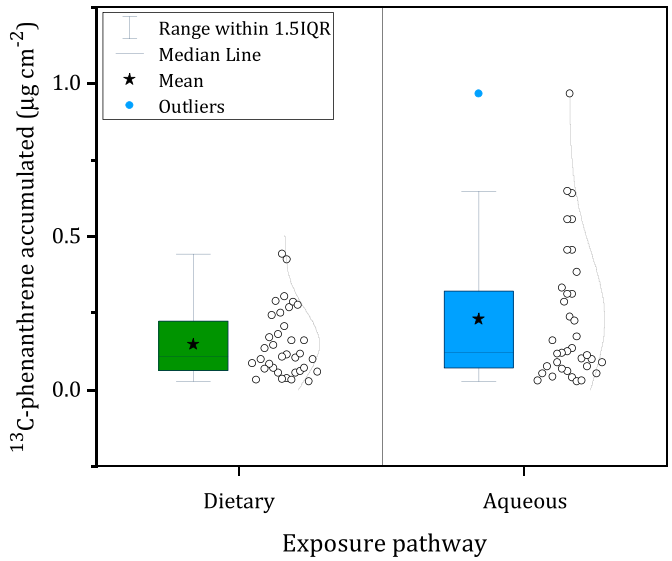

Fig. 4. Box plot of ^{13}C-phenanthrene accumulated (µg cm^{-2}) in *A. millepora* fragments via dietary (green) and aqueous (blue) exposure pathways in both treatment concentrations at the end of the experimental time. The box spans the 25% and 75% quartiles and the whiskers represent the 10% and 90% percentiles. Adjacent empty circles show raw data points with normal distribution curve. One-way ANOVA identified no significant difference in quantity of ^{13}C-phenanthrene accumulated (F-ratio = 3.72; p = 0.0576; DF = 71) between dietary and aqueous exposure. (For interpretation of the references to color in this figure legend, the reader is referred to the Web version of this article.)

studies that found mussels to accumulate significantly more dissolved ^{14}C-phenanthrene in the presence of phytoplankton, which was attributed to higher filtering rates in the presence of food particles (Björk and Gilek, 1996). In zebra fish and cichlids, the presence of prey organisms such as *Daphnia magna* elevated uptake rates of phenanthrene and other PAHs, without altering final concentrations accumulated (Xia et al., 2015). On the contrary, in corals, we found a high rate of uptake solely via diffusion, whereas, both aqueous and dietary uptake routes contributed eventually to the accumulation of similar tissue concentrations of phenanthrene. We also observed lower variability in dietary treatments. Although more consistent uptake from feeding than from seawater seems counterintuitive, feeding rates for corals have previously shown to be consistent (Anthony, 2000; Leal et al., 2014; Orejas et al., 2016), and it is possible that differences in the fine-scale irregular surfaces of the coral colonies may contribute to variability in diffusive uptake from aqueous media, with observed faster uptake rates but also higher elimination through mechanisms such as mucus secretion (Loya and Rinkevich, 1980; Mitchell and Chet, 1975). Hydrophobic contaminants, once bioconcentrated in phytoplankton, are known to have limited or slow desorption rates (Koelmans, 2014). Hence, despite lower uptake rates, PAHs acquired through dietary exposure may be retained for longer eventually resulting in similar accumulation levels.

The similar accumulation levels observed from both exposure routes were also reflected in the log BCF values which showed only a minor difference between aqueous (log BCF = 3.72) and dietary exposure (log BCF = 3.58) routes. Coral BCF estimated in this experiment is a factor higher than reported log BCFs for nematodes (2.92) (Spann et al., 2015), freshwater isopods (2.8 ± 0.5) (Van Hattum and Cid Montanes, 1999) and aligns closer to those estimated for certain copepod species (3.80, *Pseudodiaptomus marinus* (Arias et al., 2016); 3.18 *Calanus finimarichus* (Jensen et al., 2012)) and larval stages of fish (3.90, *Danio rerio*) (Petersen and Kristensen, 1998; Xia et al., 2015). The coral BCF is lower than octanol-water partition co-efficient of phenanthrene (K_{ow} = 4.53) indicating the likelihood of some elimination mechanisms (Jensen et al., 2012).

Furthermore, the toxicity of pollutants to marine biota through

dietary exposure is substantially less documented (Wang and Wang, 2014; Wang et al., 2017). In this study, we also looked at the toxicity of ^{13}C-phenanthrene to corals at tested experimental concentrations (18.2, 44 μg L^{-1}). Although the concentrations that corals were exposed to in this study are a factor higher than reported oceanic concentrations (Smith et al., 1987), there is a lack of routine monitoring near coral reefs, and it is likely that higher concentrations would be found in the proximity of oil spills, effluent plumes and contaminated shorelines (Hutchings and Haynes, 2000; Kroon et al., 2019; Mojiri et al., 2019). The concentrations applied here are comparable to those used with radioactive labelled chemicals (^{14}C-phenanthrene) to study uptake (Solbakken et al., 1984; Spann et al., 2015). The accumulation in coral tissue in the present study is higher than reported concentrations in wild coral tissue (Ko et al., 2014; Xiang et al., 2018). Nonetheless, studies indicate that the toxicity of individual PAHs vary greatly. For example, a recent study on the effects of phenanthrene showed slightly reduced coral larval settlement and no mortality at the concentrations tested here (Overmans et al., 2018), while the PAH anthracene affected both survival and settlement at far lower concentrations in the same study. The low apparent toxicity of phenanthrene to adult corals here (no effects on mortality or photosynthesis), supports the notion that larvae are more sensitive to PAHs than adult corals (Negri et al., 2016; Renegar et al., 2017).

5. Conclusion

Through a novel application of CRDS, we have traced accumulation and transfer of a model oil-derived contaminant, ^{13}C-phenanthrene in a coral reef food-chain. Our findings emphasize that both dissolved and dietary routes of exposure can contribute (similarly in this case) to the total accumulation of PAHs in coral tissue. This finding has important consequences for understanding pollutant dynamics in tropical marine food webs and draws attention to the need for including trophic transfer as a critical aspect in the risk assessment of pollutants. Foreseeably, the CRDS method could extend to complex food-web experiments, and be applied to other organic pollutants that concern aquatic-marine ecosystems.

CRediT authorship contribution statement

Ananya Ashok: Methodology, Investigation, Formal analysis, Visualization, Writing - original draft, Writing - review & editing. **Sreejith Kottuparambil:** Methodology, Investigation, Writing - review & editing. **Lone Høj:** Conceptualization, Funding acquisition, Methodology, Writing - review & editing. **Andrew P. Negri:** Conceptualization, Funding acquisition, Methodology, Writing - review & editing. **Carlos M. Duarte:** Conceptualization, Funding acquisition, Methodology, Writing - review & editing. **Susana Agustí:** Conceptualization, Funding acquisition, Methodology, Formal analysis, Writing - original draft, Writing - review & editing.

Acknowledgements

This research was funded by King Abdullah University of Science and Technology (KAUST) through baseline funding to S. Agustí, start-up funding to C.M. Duarte and a center partnership project between the Red Sea Research Center (RSRC) and the Australian Institute of Marine Science (AIMS). This research also benefited from resources of the Core Labs of King Abdullah University of Science and Technology (KAUST). We thank Florita Flores, Diane Brinkman and Biying Wu for their help in conducting the experiments, SeaSim staff at AIMS for providing their expertise and assistance, and Paloma Carrillo de Albornoz for help with Picarro-CRDS analysis.

References

Anthony, K.R.N., 2000. Enhanced particle-feeding capacity of corals on turbid reefs (Great Barrier Reef, Australia). Coral Reefs 19, 59–67. https://doi.org/10.1007/s003380050227.
Anthony, K.R.N., 1999. Coral suspension feeding on fine particulate matter. J. Exp. Mar. Biol. Ecol. 232, 85–106. https://doi.org/10.1016/S0022-0981(98)00099-9.
Arias, A.H., Souissi, A., Roussin, M., Ouddane, B., Souissi, S., 2016. Bioaccumulation of PAHs in marine zooplankton: an experimental study in the copepod *Pseudodiaptomus marinus*. Environ. Earth Sci. 75, 1–9. https://doi.org/10.1007/s12665-016-5472-1.
Ayukai, T., 1995. Retention of phytoplankton and planktonic microbes on coral reefs within the Great Barrier Reef, Australia. Coral Reefs 14, 141–147. https://doi.org/10.1007/BF00367231.
Bernard, L., Mougel, C., Maron, P., Nowak, V., Lévêque, J., Henault, C., Haichar, Z., Berge, O., Marol, C., Balesdent, J., Gibiat, F., Lemanceau, P., Ranjard, L., 2007. Dynamics and identification of soil microbial populations actively assimilating carbon from ^{13}C-labelled wheat residue as estimated by DNA- and RNA-SIP techniques. Environ. Microbiol. 9, 752–764. https://doi.org/10.1111/j.1462-2920.2006.01197.x.
Berrojalbiz, N., Lacorte, S., Calbet, A., Saiz, E., Barata, C., Dachs, J., 2009. Accumulation and cycling of polycyclic aromatic hydrocarbons in zooplankton. Environ. Sci. Technol. 43, 2295–2301. https://doi.org/10.1021/es8018226.
Bier, D.M., 1997. Stable isotope tracers: technological tools that have emerged. In: Carlson-Newberry, S.J., Costello, R.B. (Eds.), Emerging Technologies for Nutrition Research. National Academy Press, Washington D.C, pp. 201–215. https://doi.org/10.17226/5827.
Björk, M., Gilek, M., 1996. Uptake and elimination of ^{14}C-phenanthrene by the blue mussel *Mytilus edulis* L. at different algal concentrations. Bull. Environ. Contam. Toxicol. 56, 151–158. https://doi.org/10.1007/s001289900022.
Bresler, V., Bissinger, V., Abelson, A., Dizer, H., Sturm, A., Kratke, R., Fishelson, L., Hansen, P.D., 1999. Marine molluscs and fish as biomarkers of pollution stress in littoral regions of the Red Sea, Mediterranean Sea and North Sea. Helgol. Mar. Res. 53, 219–243. https://doi.org/10.1007/s101520050026.
Bustamante, P., Luna-Acosta, A., Clemens, S., Cassi, R., Thomas-Guyon, H., Warnau, M., 2012. Bioaccumulation and metabolisation of ^{14}C-pyrene by the Pacific oyster *Crassostrea gigas* exposed via seawater. Chemosphere 87, 938–944. https://doi.org/10.1016/j.chemosphere.2012.01.049.
Carrasco Navarro, V., Leppänen, M.T., Kukkonen, J.V.K., Godoy Olmos, S., 2013. Trophic transfer of pyrene metabolites between aquatic invertebrates. Environ. Pollut. 173, 61–67. https://doi.org/10.1016/j.envpol.2012.09.023.
Casserly, D.M., Davis, E.M., Downs, T.D., Guthrie, R.K., 1983. Sorption of organics by *Selenastrum capricornutum*. Water Res. 17, 1591–1594.
Cennerazzo, J., de Junet, A., Audinot, J.N., Leyval, C., 2017. Dynamics of PAHs and derived organic compounds in a soil-plant mesocosm spiked with ^{13}C-phenanthrene. Chemosphere 168, 1619–1627. https://doi.org/10.1016/j.chemosphere.2016.11.145.
Chen, H., Zhang, Z., Tian, F., Zhang, L., Li, Y., Cai, W., Jia, X., 2018. The effect of pH on the acute toxicity of phenanthrene in a marine microalgae *Chlorella salina*. Sci. Rep. 8, 1–8. https://doi.org/10.1038/s41598-018-35686-9.
Di Toro, D.M., McGrath, J.A., Hansen, D.J., 2000. Technical basis for narcotic chemicals and polycyclic aromatic hydrocarbon criteria. I. Water and tissue. Environ. Toxicol. Chem. An Int. J. 19, 1951–1970.
Echeveste, P., Agustí, S., Dachs, J., 2010. Cell size dependent toxicity thresholds of polycyclic aromatic hydrocarbons to natural and cultured phytoplankton populations. Environ. Pollut. 158, 299–307. https://doi.org/10.1016/j.envpol.2009.07.006.
Fan, C.W., Reinfelder, J.R., 2003. Phenanthrene accumulation kinetics in marine diatoms. Environ. Sci. Technol. 37, 3405–3412. https://doi.org/10.1021/es026367g.
Freitag, D., Ballhorn, L., Geyer, H., Korte, F., 1985. Environmental hazard profile of organic chemicals: an experimental method for assessment of the behaviour of organic chemicals in the ecosphere by means of simple laboratory tests with ^{14}C labelled chemicals. Chemosphere 14, 1589–1616.
French-McCay, D.P., 2002. Development and application of an oil toxicity and exposure model. OilToxEx. Environ. Toxicol. Chem. 21, 2080–2094.
Gerofke, A., Kömp, P., McLachlan, M.S., 2005. Bioconcentration of persistent organic pollutants in four species of marine phytoplankton. Environ. Toxicol. Chem. 24, 2908–2917. https://doi.org/10.1897/04-566R.1.
Geyer, H.J., Scheunert, I., Brüggemann, R., Steinberg, C., Korte, F., Kettrup, A., 1991. QSAR for organic chemical bioconcentration in *Daphnia*, algae, and mussels. Sci. Total Environ. 109, 387–394. https://doi.org/10.1016/0048-9697(91)90193-I.
Graeve, M., Albers, C., Kattner, G., 2005. Assimilation and biosynthesis of lipids in Arctic Calanus species based on feeding experiments with a ^{13}C labelled diatom. J. Exp. Mar. Biol. Ecol. 317, 109–125. https://doi.org/10.1016/j.jembe.2004.11.016.
Graham, W.M., Condon, R.H., Carmichael, R.H., D'ambra, I., Patterson, H.K., Linn, L.J., Hernandez, F.J., 2010. Oil carbon entered the coastal planktonic food web during the Deepwater Horizon oil spill. Environ. Res. Lett. 5. https://doi.org/10.1088/1748-9326/5/4/045301.
Halling-Sørensen, B., Nyholm, N., Kusk, K.O., Jacobsson, E., 2000. Influence of nitrogen status on the bioconcentration of hydrophobic organic compounds to *Selenastrum capricornutum*. Ecotoxicol. Environ. Saf. 45, 33–42. https://doi.org/10.1006/eesa.1999.1818.
Houlbrèque, F., Tambutté, E., Richard, C., Ferrier-pagès, C., 2004. Importance of a micro-diet for scleractinian corals. Mar. Ecol. Prog. Ser. 282, 151–160.
Hughes, T.P., Kerry, J.T., Álvarez-Noriega, M., Álvarez-Romero, J.G., Anderson, K.D., Baird, A.H., Babcock, R.C., Beger, M., Bellwood, D.R., Berkelmans, R., Bridge, T.C., Butler, I.R., Byrne, M., Cantin, N.E., Comeau, S., Connolly, S.R., Cumming, G.S.,

Dalton, S.J., Diaz-Pulido, G., Eakin, C.M., Figueira, W.F., Gilmour, J.P., Harrison, H.B., Heron, S.F., Hoey, A.S., Hobbs, J.P.A., Hoogenboom, M.O., Kennedy, E.V., Kuo, C.Y., Lough, J.M., Lowe, R.J., Liu, G., McCulloch, M.T., Malcolm, H.A., McWilliam, M.J., Pandolfi, J.M., Pears, R.J., Pratchett, M.S., Schoepf, V., Simpson, T., Skirving, W.J., Sommer, B., Torda, G., Wachenfeld, D.R., Willis, B.L., Wilson, S.K., 2017. Global warming and recurrent mass bleaching of corals. Nature 543, 373–377. https://doi.org/10.1038/nature21707.

Hutchings, P., Haynes, D., 2000. Sources, fates and consequences of pollutants in the Great Barrier Reef. Mar. Pollut. Bull. 41 (7–12), 265–266. https://doi.org/10.1016/S0025-326X(00)00143-0.

Jafarabadi, A.R., Bakhtiari, A.R., Aliabadian, M., Laetitia, H., Toosi, A.S., Yap, C.K., 2018. First report of bioaccumulation and bioconcentration of aliphatic hydrocarbons (AHs) and persistent organic pollutants (PAHs, PCBs and PCNs) and their effects on alcyonacea and scleractinian corals and their endosymbiotic algae from the Persian Gulf, Iran. Sci. Total Environ. 627, 141–157. https://doi.org/10.1016/j.scitotenv.2018.01.185.

Jensen, L.K., Honkanen, J.O., Jæ, ger, I., Carroll, J.L., 2012. Bioaccumulation of phenanthrene and benzo[a]pyrene in *Calanus finmarchicus*. Ecotoxicol. Environ. Saf. 78, 225–231. https://doi.org/10.1016/j.ecoenv.2011.11.029.

Kennedy, C.J., Gassman, N.J., Walsh, P.J., 1992. The fate of benzo[a]pyrene in the scleractinian corals *Favia fragum* and *Montastrea annularis*. Mar. Biol. 113, 313–318.

Kennish, M.J., 2017. Practical Handbook of Estuarine and Marine Pollution. CRC Press, Boca Rotan. https://doi.org/10.1201/9780203742488.

Knap, A.H., Solbakken, J.E., Dodge, R.E., Sleeter, T.D., Wyers, S.J., Palmork, K.H., 1982. Accumulation and elimination of ($^{9\text{-}14}$C) phenanthrene in the reef-building coral (*Diploria strigosa*). Bull. Environ. Contam. Toxicol. 28, 281–284. https://doi.org/10.1007/BF01608508.

Ko, F.C., Chang, C.W., Cheng, J.O., 2014. Comparative study of polycyclic aromatic hydrocarbons in coral tissues and the ambient sediments from Kenting National Park, Taiwan. Environ. Pollut. 185, 35–43. https://doi.org/10.1016/j.envpol.2013.10.025.

Koelmans, A.A., 2014. Limited reversibility of bioconcentration of hydrophobic organic chemicals in phytoplankton. Environ. Sci. Technol. 48, 7341–7348. https://doi.org/10.1021/es5003549.

Kroon, F.J., Berry, K.L.E., Brinkman, D.L., Kookana, R., Leusch, F.D.L., Melvin, S.D., Neale, P.A., Negri, A.P., Puotinen, M., Tsang, J.J., van de Merwe, J.P., Williams, M., 2019. Sources, presence, and potential effects of contaminants of emerging concern in the marine environments of the Great Barrier Reef and Torres Strait, Australia. Sci. Total Environ (in press).

Leal, M.C., Ferrier-Pagès, C., Calado, R., Thompson, M.E., Frischer, M.E., Nejstgaard, J.C., 2014. Coral feeding on microalgae assessed with molecular trophic markers. In: Molecular Ecology, pp. 3870–3876. https://doi.org/10.1111/mec.12486.

Limer, L.M.C., Le Dizès-Maurel, S., Klos, R., Maro, D., Nordén, M., 2015. Impacts of ^{14}C discharges from a nuclear fuel reprocessing plant on surrounding vegetation: comparison between grass field measurements and TOCATTA-χ and SSPAM14C model computations. J. Environ. Radioact. 147, 115–124. https://doi.org/10.1016/j.jenvrad.2015.05.015.

López-Sandoval, D.C., Delgado-Huertas, A., Carrillo-de-Albornoz, P., Duarte, C.M., Agustí, S., 2019. Use of cavity ring-down spectrometry to quantify ^{13}C-primary productivity in oligotrophic waters. Limnol Oceanogr. Methods. https://doi.org/10.1002/lom3.10305.

Loya, Y., Rinkevich, B., 1980. Effects of oil pollution on coral reef communities. Mar. Ecol. Prog. Ser. 2, 167–180.

Lu, X., Reible, D.D., Fleeger, J.W., 2004. Relative importance of ingested sediment versus pore water as uptake routes for PAHs to the deposit-feeding oligochaete *Ilyodrilus templetoni*. Arch. Environ. Contam. Toxicol. 47, 207–214. https://doi.org/10.1007/s00244-004-3053-x.

Maher, D.T., Santos, I.R., Leuven, J.R.F.W., Oakes, J.M., Erler, D.V., Carvalho, M.C., Eyre, B.D., 2013. Novel use of cavity ring-down spectroscopy to investigate aquatic carbon cycling from microbial to ecosystem scales. Environ. Sci. Technol. 47, 12938–12945. https://doi.org/10.1021/es4027776.

Mallhot, H., 1987. Prediction of algal bioaccumulation and uptake rate of nine organic compounds by ten physicochemical properties. Environ. Sci. Technol. 21, 1009–1013. https://doi.org/10.1021/es50001a016.

Martinez, E., Gros, M., Lacorte, S., Barceló, D., 2004. Simplified procedures for the analysis of polycyclic aromatic hydrocarbons in water, sediments and mussels. J. Chromatogr. A 1047, 181–188. https://doi.org/10.1016/j.chroma.2004.07.003.

Mercurio, P., Eaglesham, G., Parks, S., Kenway, M., Beltran, V., Flores, F., Mueller, J.F., Negri, A.P., 2018. Contribution of transformation products towards the total herbicide toxicity to tropical marine organisms. Sci. Rep. 8, 4808. https://doi.org/10.1038/s41598-018-23153-4.

Mitchell, R., Chet, I., 1975. Bacterial attack of corals in polluted seawater. Microb. Ecol. 2, 227–233. https://doi.org/10.1007/BF02010442.

Mojiri, A., Zhou, J.L., Ohashi, A., Ozaki, N., Kindaichi, T., 2019. Comprehensive review of polycyclic aromatic hydrocarbons in water sources, their effects and treatments. Sci. Total Environ. https://doi.org/10.1016/j.scitotenv.2019.133971.

Muscatine, L., Goiran, C., Land, L., Jaubert, J., Cuif, J.P., Allemand, D., 2005. Stable isotopes (δ13C and δ15N) of organic matrix from coral skeleton. Proc. Natl. Acad. Sci. U. S. A. 102, 1525–1530. https://doi.org/10.1073/pnas.0408921102.

Naumann, M.S., Niggl, W., Laforsch, C., Glaser, C., Wild, C., 2009. Coral surface area quantification-evaluation of established techniques by comparison with computer tomography. Coral Reefs 28, 109–117. https://doi.org/10.1007/s00338-008-0459-3.

Negri, A.P., Brinkman, D.L., Flores, F., Botte, E.S., Jones, R.J., Webster, N.S., 2016. Acute ecotoxicology of natural oil and gas condensate to coral reef larvae. Sci. Rep. 6, 1–10. https://doi.org/10.1038/srep21153.

Nomaki, H., Heinz, P., Nakatsuka, T., Shimanaga, M., Kitazato, H., 2005. Species-specific ingestion of organic carbon by deep-sea benthic foraminifera and meiobenthos: in situ tracer experiments. Limnol. Oceanogr. 50, 134–146. https://doi.org/10.4319/lo.2005.50.1.0134.

Nordborg, F.M., Flores, F., Brinkman, D.L., Agustí, S., Negri, A.P., 2018. Phototoxic effects of two common marine fuels on the settlement success of the coral *Acropora tenuis*. Sci. Rep. 8, 1–12. https://doi.org/10.1038/s41598-018-26972-7.

Orejas, C., Gori, A., Rad-Menéndez, C., Last, K.S., Davies, A.J., Beveridge, C.M., Sadd, D., Kiriakoulakis, K., Witte, U., Roberts, J.M., 2016. The effect of flow speed and food size on the capture efficiency and feeding behaviour of the cold-water coral *Lophelia pertusa*. J. Exp. Mar. Biol. Ecol. 481, 34–40. https://doi.org/10.1016/j.jembe.2016.04.002.

Osinga, R., Schutter, M., Wijgerde, T., Rinkevich, B., Shafir, S., Shpigel, M., Luna, G.M., Danovaro, R., Bongiorni, L., Deutsch, A., Kuecken, M., Hiddinga, B., Janse, M., McLeod, A., Gili, C., Lavorano, S., Henard, S., Barthelemy, D., Westhoff, G., Baylina, N., Santos, E., Weissenbacher, A., Kuba, M., Jones, R., Leewis, R., Petersen, D., Laterveer, M., 2012. The CORALZOO project: a synopsis of four years of public aquarium science. J. Mar. Biol. Assoc. U. K. 92, 753–768. https://doi.org/10.1017/S0025315411001779.

Overmans, S., Nordborg, M., Díaz-rúa, R., Brinkman, D.L., Negri, A.P., Agustí, S., 2018. Phototoxic effects of PAH and UVA exposure on molecular responses and developmental success in coral larvae. Aquat. Toxicol. 198, 165–174. https://doi.org/10.1016/j.aquatox.2018.03.008.

Peters, E.C., Meyers, P.A., Yevich, P.P., Blake, N.J., 1981. Bioaccumulation and histopathological effects of oil on a stony coral. Mar. Pollut. Bull. 12, 333–339. https://doi.org/10.1016/0025-326X(81)90106-5.

Petersen, G.I., Kristensen, P., 1998. Bioaccumulation of lipophilic substances in fish early life stages. Environ. Toxicol. Chem. 17, 1385–1395. https://doi.org/10.1897/1551-5028(1998)017<1385:BOLSIF>2.3.CO.

Piccinetti, C.C., Ricci, R., Pennesi, C., Radaelli, G., Totti, C., Norici, A., Giordano, M., Olivotto, I., 2016. Herbivory in the soft coral *Sinularia flexibilis* (Alcyoniidae). Sci. Rep. 6, 1–8. https://doi.org/10.1038/srep22679.

Plant, A.L., Knapp, R.D., Smith, L.C., 1987. Mechanism and rate of permeation of cells by polycyclic aromatic hydrocarbons. J. Biol. Chem. 262, 2514–2519.

Ralph, P.J., Smith, R.A., Macinnia-Ng, C.M.O., Seery, C.R., 2007. Use of fluorescence-based ecotoxicological bioassays in monitoring toxicants and pollution in aquatic systems. Toxicol. Environ. Chem. 89, 589–607. https://doi.org/10.1080/02772240701561593.

Redman, A.D., Parkerton, T.F., 2015. Guidance for improving comparability and relevance of oil toxicity tests. Mar. Pollut. Bull. 98, 156–170.

Renegar, D.A., Turner, N.R., Riegl, B.M., Dodge, R.E., Knap, A.H., Schuler, P.A., 2017. Acute and subacute toxicity of the polycyclic aromatic hydrocarbon 1-methylnaphthalene to the shallow-water coral Porites divaricata: application of a novel exposure protocol. Environ. Toxicol. Chem. 36, 212–219. https://doi.org/10.1002/etc.3530.

Reynolds, C.S., 1984. The Ecology of Freshwater Phytoplankton. Cambridge University Press.

Richnow, H.H., Eschenbach, A., Mahro, B., Seifert, R., Wehnmg, P., Albrecht, P., Michaelis, W., Hamburg-harburg, U., Hamburg, D.-, 1998. The use of ^{13}C-labelled polycyclic aromatic hydrocarbons for the analysis of their transformation in soil. Chemosphere 36, 2211–2224.

Schaffelke, B., Carleton, J., Doyle, J., Furnas, M., Gunn, K., Skuza, M., Wright, M., Zagorskis, I., 2011. Reef Rescue Monitoring Program, Final Report of AIMS Activities 2010/11 - Inshore Water Quality Monitoring. Report for Great Barrier Reef Marine Park Authority. Australian Institute of Marine Science, Townsville.

Schreiber, U., Quayle, P., Schmidt, S., Escher, B.I., Mueller, J.F., 2007. Methodology and evaluation of a highly sensitive algae toxicity test based on multiwell chlorophyll fluorescence imaging. Biosens. Bioelectron. 22, 2554–2563. https://doi.org/10.1016/j.bios.2006.10.018.

Siebeck, U.E., Marshall, N.J., Klüter, A., Hoegh-Guldburg, O., 2006. Monitoring coral bleaching using a colour reference card. Coral Reefs 25, 453–460. https://doi.org/10.1007/s00338-006-0123-8.

Smith, J.D., Bagg, J., Sin, Y.O., 1987. Aromatic hydrocarbons in seawater, sediments and clams from green island, great barrier reef, Australia. Mar. Freshw. Res. 38, 501–510. https://doi.org/10.1071/MF9870501.

Solbakken, J., Knap, A., Sleeter, T., Searle, C., Palmork, K., 1984. Investigation into the fate of ^{14}C-labelled xenobiotics (naphthalene, phenanthrene, 2,4,5,2',4',5'-hexachlorobiphenyl, octachlorostyrene) in Bermudian corals. Mar. Ecol. Prog. Ser. 16, 149–154. https://doi.org/10.3354/meps016149.

Spann, N., Goedkoop, W., Traunspurger, W., 2015. Phenanthrene bioaccumulation in the nematode *Caenorhabditis elegans*. Environ. Sci. Technol. 49, 1842–1850. https://doi.org/10.1021/es504553t.

Sulzmann, E.W., 2007. Stable isotope chemistry and measurement: a primer. In: Michener, R., Lajtha, K. (Eds.), Stable Isotopes in Ecology and Environmental Science. Blakcwell Publishing Ltd, pp. 1–18.

Towle, E.K., Enochs, I.C., Langdon, C., 2015. Threatened Caribbean coral is able to mitigate the adverse effects of ocean acidification on calcification by increasing feeding rate. PloS One 10, 1–17. https://doi.org/10.1371/journal.pone.0123394.

Tremblay, P., Grover, R., Maguer, J.F., Legendre, L., Ferrier-Pages, C., 2012. Autotrophic carbon budget in coral tissue: a new ^{13}C-based model of photosynthate translocation. J. Exp. Biol. 215, 1384–1393. https://doi.org/10.1242/jeb.065201.

Turner, N.R., Renegar, D.A., 2017. Petroleum hydrocarbon toxicity to corals: a review. Mar. Pollut. Bull. 119, 1–16. https://doi.org/10.1016/j.marpolbul.2017.04.050.

Valdez Domingos, F.X., Oliveira Ribeiro, C.A., Pelletier, É., Rouleau, C., 2011. Tissue distribution and depuration kinetics of waterborne ^{14}C-labeled light PAHs in mummichog (*Fundulus heteroclitus*). Environ. Sci. Technol. 45, 2684–2690. https://doi.org/10.1021/es103133h.

Van Hattum, B., Cid Montanes, J.F., 1999. Toxicokinetics and bioconcentration of

polycyclic aromatic hydrocarbons in freshwater isopods. Environ. Sci. Technol. 33, 2409–2417. https://doi.org/10.1021/es9800479.

Wan, Y., Jin, X., Hu, J., Jin, F., 2007. Trophic dilution of polycyclic aromatic hydrocarbons (PAHs) in a marine food web from Bohai Bay, North China. Environ. Sci. Technol. 41, 3109–3114. https://doi.org/10.1021/es062594x.

Wang, X., Wang, W.X., 2006. Bioaccumulation and transfer of benzo(a)pyrene in a simplified marine food chain. Mar. Ecol. Prog. Ser. 312, 101–111. https://doi.org/10.3354/meps312101.

Wang, J., Wang, W., 2014. Low bioavailability of silver nanoparticles presents trophic toxicity to marine medaka (*Oryzias melastigma*). Environ. Sci. Technol. 48, 8152–8161. https://doi.org/10.1021/es500655z.

Wang, Z., Xia, B., Chen, B., Sun, X., Zhu, L., Zhao, J., Du, P., Xing, B., 2017. Trophic transfer of TiO2 nanoparticles from marine microalga (*Nitzschia closterium*) to scallop (*Chlamys farreri*) and related toxicity. Environ. Sci. Nano 4, 415–424. https://doi.org/10.1039/c6en00365f.

Xia, X., Li, H., Yang, Z., Zhang, X., Wang, H., 2015. How does predation affect the bioaccumulation of hydrophobic organic compounds in aquatic organisms? Environ. Sci. Technol. 49, 4911–4920. https://doi.org/10.1021/acs.est.5b00071.

Xiang, N., Jiang, C., Yang, T., Li, P., Wang, H., Xie, Y., 2018. Occurrence and distribution of polycyclic aromatic hydrocarbons (PAHs) in seawater , sediments and corals from Hainan Island , China. Ecotoxicol. Environ. Saf. 152, 8–15. https://doi.org/10.1016/j.ecoenv.2018.01.006.

Yakan, S.D., Henkelmann, B., Schramm, K.W., Okay, O.S., 2013. Bioaccumulation - depuration kinetics and effects of phenanthrene on Mediterranean mussel (*Mytilus galloprovincialis*). J. Environ. Sci. Heal. - Part A Toxic/Hazardous Subst. Environ. Eng. 48, 1037–1046. https://doi.org/10.1080/10934529.2013.773799.

Yang, T., Cheng, H., Wang, H., Drews, M., Li, S., Huang, W., Zhou, H., Min, C., Diao, X., 2019. Comparative study of polycyclic aromatic hydrocarbons (PAHs) and heavy metals (HMs) in corals, surrounding sediments and surface water at the Dazhou Island, China. Chemosphere 218, 157–168. https://doi.org/10.1016/j.chemosphere.2018.11.063.